Acta Cryst. (1985). B41, 411-418

A Model Structure for the $Al_{5-x}Ti_{3+x}$ Phase using High-Resolution Electron Microscopy

BY A. LOISEAU AND A. LASALMONIE

Office National d'Etudes et de Recherches Aérospatiales (ONERA), BP 72 92322 Chatillon CEDEX, France

AND G. VAN TENDELOO, J. VAN LANDUYT AND S. AMELINCKX*

RUCA Groenenborgerlaan 171, B-2020 Antwerp, Belgium

(*Received 25 June 1984; accepted 14 June 1985*)

Abstract

Electron diffraction patterns of Al-Ti alloys show incommensurate as well as commensurate superstructure spots depending on the nominal composition ranging from Al-37 at.% Ti to Al-44 at.% Ti. It is shown that the alloy has a heterogeneous structure constituted of island-like precipitates in the matrix of AlTi ($L1_0$ structure) and that the incommensurability depends upon the size of the island which decreases with Al content in the alloy. A model structure is proposed from the optical analysis of high-resolution images obtained at 200 kV: each island of the Al_5Ti_3 core is surrounded by a third phase having an intermediate composition which is assumed to be $Al_{11}Ti_7$. Optical simulation of the electron diffraction pattern is tried using plane masks representing the islands of various sizes.

1. Introduction

Recently a new type of ordered structure, based on the face-centered cubic lattice, has been reported in Al-Ti and Ga-Ti alloys by Miida, Hashimoto & Watanabe (1982) and by Loiseau & Lasalmonie (1983). In both cases the interpretation was mainly based on electron diffraction data. According to Miida *et al.* (1982) the structure is commensurate, and has tetragonal symmetry; it is discussed below in further detail.

Loiseau & Lasalmonie (1983), on the other hand, in Al-Ti alloys with compositions in the range from 42 to 44 at.% Ti observed rather similar diffraction patterns, which were, however, slightly incommensurate. These incommensurate diffraction patterns were previously interpreted as a superposition of the diffraction patterns of two different structures, both partly coherent with the AlTi matrix ($L1_0$-type structure) and derived from this by introduction of antiphase boundaries along {110} planes. Such a structure may give rise to the incommensurability of certain superstructure spots. However, dark-field images in these superstructure reflections failed to reveal domain structures, as would be the case if different structures were present. This was attributed to the small size of the domains (≤ 10 nm). Using high-resolution electron microscopy and optical diffraction on alloys containing 37-44 at.% Ti, we arrived at the conclusion that all the superstructure spots, commensurate and incommensurate, must originate from the same structure. This forced us to re-interpret some of the observations, bearing in mind that pseudo-incommensurate diffraction patterns may result from the mixing of different spacings.

2. Structural considerations

We shall describe the superstructure reported by Miida *et al.* (1982) since this structure will be the basis for a detailed understanding of the observed incommensurabilities. The structure is based on an f.c.c. lattice, the base vectors of the tetragonal lattice being:

$$Al_5Ti_3: \begin{vmatrix} \mathbf{a}_1' \\ \mathbf{a}_2' \\ \mathbf{a}_3' \end{vmatrix}_{\text{tetr.}} = \begin{vmatrix} 2 & 2 & 0 \\ 2 & -2 & 0 \\ 0 & 0 & 1 \end{vmatrix} \begin{vmatrix} \mathbf{a}_1 \\ \mathbf{a}_2 \\ \mathbf{a}_3 \end{vmatrix}_{\text{f.c.c.}}$$

The structure can be described as a Ti-deficient AlTi superstructure (CuAu type) with ideal composition Al_5Ti_3. In the AlTi structure cube planes perpendicular to the tetragonal axis are alternately occupied exclusively by Ti and Al. In the Al_5Ti_3 superstructure, the Al planes are conserved but some of the Ti atoms are replaced by Al atoms giving rise to a succession of pure Al planes and planes with a mixed composition $AlTi_3$. The geometry of such a mixed plane is represented in Fig. 1(*a*). Another representation of this structure is given in Fig. 1(*b*). Outside the centered unit cell only the Al atoms are represented; the remaining f.c.c. sites in this plane are occupied by Ti. This representation will be useful when comparing the high-resolution images with the structural model.

A second structure, a hypothetical one but important for the later interpretation, has a composition $Al_{11}Ti_7$, *i.e.* slightly more Ti-rich than Al_5Ti_3. This also consists of alternating pure Al (001) planes and mixed planes with composition Al_2Ti_7 (as compared

* Also at SCK/CEN Mol, Belgium.

0108-7681/85/060411-08$01.50

to Al_2Ti_6 for the Al_5Ti_3 structure). The geometry of such a mixed plane is represented in Fig. 1(*c*); only Al atoms are represented outside the projected unit cell, the remaining f.c.c. sites being occupied by Ti.

The tetragonal unit cell can be chosen either as primitive or as *C*-face centered (Fig. 1*c*). The base vectors of the primitive unit cell are given by

$$Al_{11}Ti_7: \begin{vmatrix} \mathbf{a}_1'' \\ \mathbf{a}_2'' \\ \mathbf{a}_3'' \end{vmatrix} = \begin{vmatrix} 3 & 0 & 0 \\ 0 & 3 & 0 \\ 0 & 0 & 1 \end{vmatrix} \begin{vmatrix} \mathbf{a}_1 \\ \mathbf{a}_2 \\ \mathbf{a}_3 \end{vmatrix}_{\text{f.c.c.}}.$$

3. The reciprocal lattice

The reciprocal lattice of the Al_5Ti_3 structure is represented in Fig. 2(*a*) by the full dots. The superstructure spots occur in square arrangements rotated 45° with respect to the cube directions, separated by diagonal lines along which all superstructure spots except 400 are absent. It becomes evident why this is so upon noting that the occupancy of all $\{110\}_{\text{f.c.c.}}$ planes is identical so that the period of the stacking of these planes is $(1/2)\sqrt{2}a_0$. However, spots along these diagonal lines can be produced at the positions marked by small open dots, as a result of double diffraction.

The most intense spots of the reciprocal lattice of the hypothetical $Al_{11}Ti_7$ structure are represented in Fig. 2(*b*) by the open dots. In this case also the superstructure spots form square arrangements centered on the same site (*e.g.* 100 spots) but now with their sides parallel to the cube directions. When the basic spots are superposed on those of Al_5Ti_3 the open dots are alternately inside and outside along the periphery of the square of full dots (Fig. 2*c*).

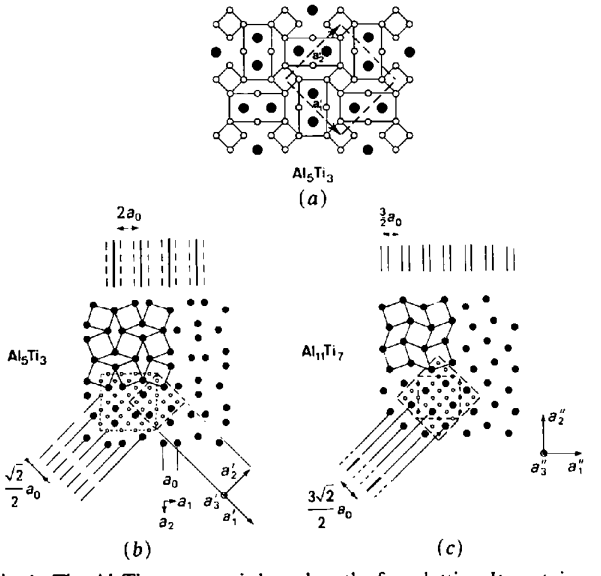

Fig. 1. The Al_5Ti_3 structure is based on the f.c.c. lattice. It contains pure Al planes at the $\frac{1}{2}$ and mixed planes at the 0 level. The diagram in (*a*) represents a mixed (001) layer; the full dots are Al, whereas the open dots are Ti. In (*b*) outside the centered unit cell only the Al positions are shown. (*c*) The hypothetical $Al_{11}Ti_7$ structure; outside the unit cell only Al atoms in mixed layers are represented. The bars represent the Al occupancy; a_0 is the f.c.c. lattice parameter ($a_0 \approx 0{\cdot}40$ nm).

4. Experimental

Alloys with compositions between 37 and 44 at.% Ti were prepared by repeated arc melting under argon atmosphere. The ingots were homogenized under vacuum ($<1{\cdot}3\times10^{-4}$Pa) at 1573 ± 1 K and ordered at 1373 ± 1 K for periods varying between 80 and 360 h. Foils for electron microscopy were obtained by electropolishing using a mixture of perchloric acid and acetic acid at 230 K.

High-resolution images were obtained using JEOL 200CX electron microscopes with a top-entry stage at the University of Antwerp (Belgium) and at the University of California, Berkeley (USA) as well as with the 1 MeV ARM microscope at Berkeley. The resolution of these instruments is of the order of 0·25 nm for the former and 0·2 nm, or somewhat better, for the latter.

The preparation of the foils is critical and the foil thickness should be as small as feasible for two reasons. In thick specimens different 'islands' or precipitates would overlap. The electropolishing method used here produces specimens with large plateaus of uniform thickness which end abruptly; no wedge-shaped edges are formed which gradually decrease in thickness. Only rarely are such plateau-shaped areas of the order of 5 to 10 nm thick and thus thin enough for high-resolution work.

5. Observations

5.1. *Diffraction patterns*

Three [001] zone-axis patterns obtained from alloys with compositions Al-37at.% Ti, Al-42 at.% Ti and Al-44 at.% Ti are reproduced in Figs. 3(*a*), 3(*b*) and 3(*c*), respectively.

In the alloy with composition Al-37 at.% Ti the reflections are at commensurate positions; this

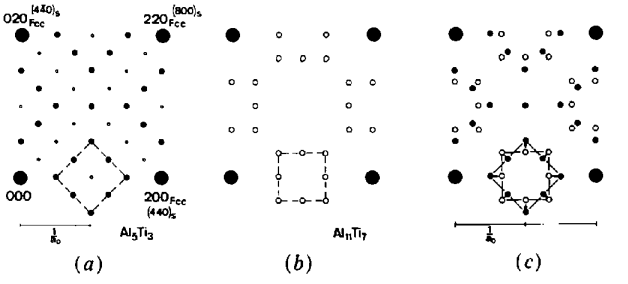

Fig. 2. *hk*0 reciprocal-lattice sections. (*a*) Al_5Ti_3 structure according to Miida *et al.* (1982). (*b*) Hypothetical $Al_{11}Ti_7$ structure. (*c*) Superposed reciprocal-lattice planes [(*a*)+(*b*)]. Large full circles indicate the f.c.c. reflections and small ones superstructure spots of which open circles represent the forbidden reflections.

diffraction pattern is the same as that obtained by Miida *et al.* (1982).

In the alloy with composition Al-42 at.% Ti the superstructure reflections appear to be shifted slightly away from the commensurate positions (Fig. 3*b*); the magnitude of the shift depends on the composition and increases with decreasing Al content as is the case for Al-44 at.% Ti (Fig. 3*c*). Fig. 4 is a schematic representation of the observed commensurate and 'incommensurate' diffraction patterns in their relative positions. The full dots represent the commensurate diffraction pattern whereas the open dots refer to the incommensurate one. The indices marked *s* refer to the Al_5Ti_3 superstructure. The spot displacements are thus evident. The displacement of the superstructure spots takes place along the lines passing through the center of the square. We choose δ as a measure of the incommensurability.

Notice also the intense 110-type spots; they are due to the presence of the AlTi structure as we shall see.

Especially in commensurate diffraction patterns double-diffraction spots are sometimes present along the diagonal lines completing in this way the square array (Fig. 3*a*).

In the incommensurate diffraction pattern double-diffraction spots are only very exceptionally present. In this case they are split, giving an indication of the magnitude of the incommensurability (Fig. 3*c*).

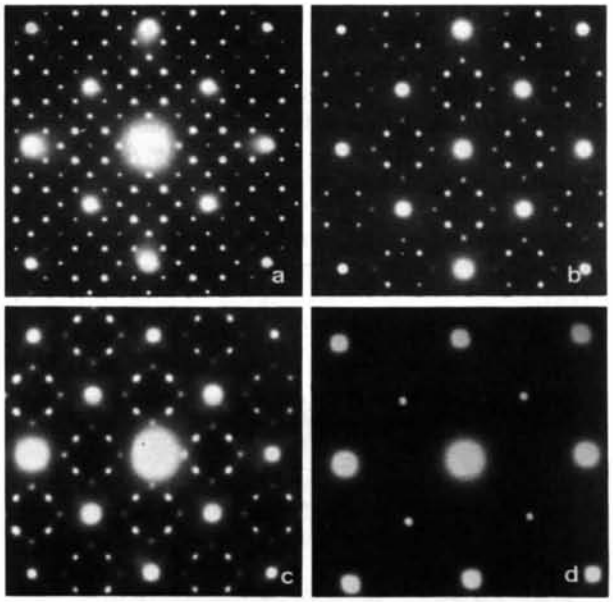

Fig. 3. Electron diffraction patterns from Al-Ti alloys (200 kV): (*a*) Al-37 at.% Ti: commensurate diffraction pattern; (*b*) Al-42 at.% Ti: weakly incommensurate diffraction pattern; (*c*) Al-44 at.% Ti: more strongly incommensurate pattern. Note the presence of split double-diffraction spots along the diagonals of the square of f.c.c. spots. (*d*) Diffraction pattern of the alloy after 1 MeV electron irradiation; only the Al-Ti spots remain visible after 10 mn at $\sim 10^{21}$ e m^{-2} s^{-1}.

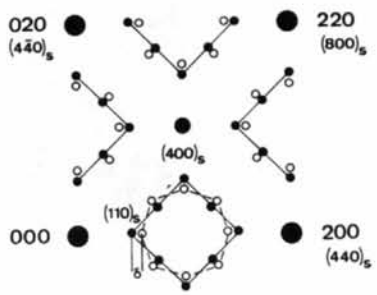

Fig. 4. Schematic representation of the relation between the diffraction patterns of the commensurate (full dots) and the 'incommensurate' structures (open dots).

5.2. *Diffraction-contrast experiments*

Using the diffraction-contrast mode we have obtained dark-field images in a single superlattice spot of the commensurate and incommensurate diffraction patterns. In isostructural Ga_5Ti_3 the whole specimen is found to contribute to such a spot. This is no longer true in Al_5Ti_3 specimens. In this case the intensity in the superlattice spots originates from small islands in the specimen (Fig. 5*a*). When making a dark-field image by one of the basic reflections to which the AlTi structure makes the main contribution, one finds on the contrary that the matrix as well as the islands light up. These observations show that this material is a two-phase system, consisting of an AlTi matrix in which islands of the superstructure are embedded. We shall subsequently refine this picture to account for the details of the observations.

The size of the islands remains small even after lengthy annealing; it decreases with increasing deviation from the A_5B_3 composition.

In stoichiometric Al_5Ti_3, which produces a commensurate diffraction pattern, with double-diffraction spots completing the square array, the islands are largest with sizes up to 50 to 100 nm. In particular, the islands now touch one another so as to give rise to coalescence and possibly overlap in projection, along their periphery (Fig. 5*b*). The double-diffraction spots originate from such overlapping parts.

5.3. *High-resolution images and their optical diffraction patterns*

5.3.1. *The* Al-37 at.% Ti *phase* (*type* I *alloy*). The most informative zone axis for high-resolution imaging is the [001] zone of Al_5Ti_3; along this direction the superlattice unit cell is only one f.c.c. unit cell thick and only atoms of the same species overlap, *i.e.* the structure is a 'column structure' in the sense defined by Van Tendeloo & Amelinckx (1978). All images were obtained in the bright-field imaging mode using a large objective aperture, the size of which is indicated in the inset of Fig. 6.

At low magnification the dot pattern is not uniform over large areas. The specimen seems to consist of a large number of small islands (*e.g.* like those encircled in Fig. 6*a*) embedded in a matrix. This is consistent with the dark-field images (Fig. 5); these are the islands having the Al_5Ti_3 superstructure.

In the very thin areas, where we expect neighboring islands not to overlap, we note the presence of a square dot configuration with a lattice parameter of ~0·28 nm, the dense rows being at less than 45° with respect to the cube directions. This is the configuration of dots to be expected for the [001] projection of the $L1_0$ structure of AlTi.

In the central part of the islands at high magnification one recognizes the presence of bright dots with enhanced brightness. The configuration and spacing of the brighter dots is sometimes the same as that of the Al-atom columns in the mixed layer of the Al_5Ti_3 structure in Fig. 1(*b*).

Computer image simulations based on the method proposed by Van Dyck (1980) and performed for thickness values between 2 and 20 nm confirm this interpretation.

The rows of bright dots are out of phase in different islands, as can be judged by looking along the rows at grazing incidence.

Often no well defined bright-dot configuration can be distinguished because of the superposition of images due to different islands.

Optical diffraction of high-resolution images allows the selection of much smaller areas than does conventional electron diffraction. In this way it is found that the central part of the larger islands has indeed the commensurate Al_5Ti_3 structure, since it produces the optical diffraction pattern reproduced in Fig. 7(*a*).

5.3.2. *The* Al–42–44 at.% Ti *phase* (*type* II *alloy*). A high-resolution image of a specimen exhibiting an incommensurate diffraction pattern is reproduced at low magnification in Fig. 8(*a*), and at high magnification in Fig. 8(*b*). The island size is visibly smaller and regions exhibiting the Al_5Ti_3 structure are smaller as well.

Optical diffraction from areas covering the boundary region of the islands, *i.e.* the transition region between the Al_5Ti_3 structure and the AlTi matrix, produces incommensurate diffraction patterns (Fig. 7*b*).

It is reasonable to suppose that the incommensurate electron diffraction patterns also originate from such areas, the difference being that the electron diffraction pattern is the average over several islands, whereas

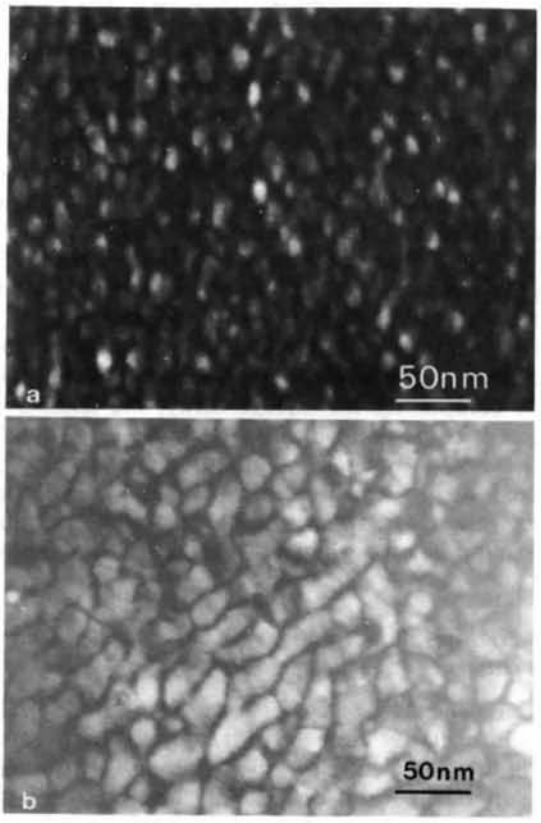

Fig. 5. Dark-field image from one of the superstructure spots. (*a*) Incommensurate diffraction pattern; only small islands light up in the matrix. (*b*) Commensurate diffraction patterns. The islands are larger. The coalescence is advanced between well developed islands. Under these conditions double-diffraction spots can be produced.

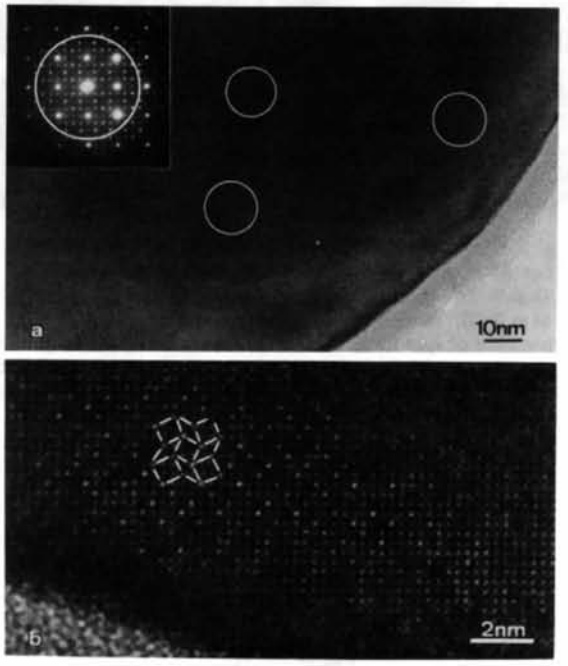

Fig. 6. High-resolution images of Al_5Ti_3 structure (200 kV). (*a*) Low-magnification image. Note the presence of large islands exhibiting bright-dot configurations differing from those in the surrounding matrix. (*b*) High-magnification image; note the correspondence between the configuration of bright dots and that of the Al atoms in Fig. 1(*b*).

the optical diffraction is due to a single island. The high-magnification image reveals configurations of brighter spots which are rather similar to those observed at the centers of the large islands. However, whereas in the central parts only squares and lozenges of bright spots of a certain type are observed, one occasionally also observes lozenges of a different type in the transition region suggesting the presence of building elements like those occurring in the hypothetical phase $Al_{11}Ti_7$ (Fig. 8*b*).

Likewise, optical diffraction allows one to conclude that the matrix of specimens giving incommensurate diffraction patterns has the $L1_0$ structure; the optical diffraction pattern of such an area is reproduced in Fig. 7(*c*).

6. Analysis of the observed diffraction patterns

It has previously been shown (Fujiwara, 1957) that diffraction patterns, exhibiting fairly sharp spots at incommensurate positions, may be produced by periodic antiphase-boundary structures as a result of the presence of a 'regular' mixture of two spacings between the antiphase boundaries. In such a case the diffraction pattern exhibits the average spacing, which may be incommensurate with respect to the basic f.c.c. lattice.

The same principle can be applied to sequences containing mixtures of two interplanar spacings such as occur in $Al_{11}Ti_7$ and Al_5Ti_3 bands separated by APB's, as suggested by Fig. 10. In this case, an average period will also result which is in general 'incommensurate' (Van Dyck, Van Tendeloo & Amelinckx, 1984).

From a comparison of the observed incommensurate diffraction patterns of Fig. 3(*c*) and the superposed theoretical diffraction patterns of the Al_5Ti_3 and $Al_{11}Ti_7$ structures (Fig. 2*c*) it is clear that the observed incommensurate spots are located between the open and full dots in Fig. 2(*c*); small shifts in the sense and direction as indicated by arrows have occurred.

This remark suggests that the incommensurate diffraction pattern may be due to a structure consisting of a mixture of unit cells belonging to the two structures discussed above, *i.e.* to the Al_5Ti_3 and the $Al_{11}Ti_7$ structures, leading to an intermediate average period.

This can also be seen by considering the family of $\{100\}_{\text{f.c.c.}}$ lattice planes. In the Al_5Ti_3 structure the period is $2a_0$ whereas in $Al_{11}Ti_7$ the corresponding period is $\frac{3}{2}a_0$ (Fig. 1*b*, *c*). Mixing rows of unit cells belonging to the two structures would lead to an average spacing somewhere between these two values depending on the number of rows of structure elements belonging to each structure (Fig. 1*b*, *c*).

It is convenient to introduce a measure for the incommensurability δ defined as the displacement of the $(110)Al_5Ti_3$ spot towards the nearest $Al_{11}Ti_7$ spot (Fig. 4). The other spot shifts are then unambiguously defined as well. The extreme values of δ are zero, corresponding to the pure Al_5Ti_3 structure, and $\frac{1}{6}$ corresponding to the pure $Al_{11}Ti_7$ structure (Fig. 2*c*). Calling p and q, respectively, the number of $Al_{11}Ti_7$ and Al_5Ti_3 structural elements one obtains for the average period $[(3/2)a_0p+2a_0q]/(p+q)$ and

$$\delta=\left[\frac{p+q}{(3/2)p+2q}-\frac{1}{2}\right]\frac{1}{a_0}=\left[\frac{1}{6+8(q/p)}\right]\frac{1}{a_0}.$$

We have seen above that the Al_5Ti_3 structure occurs in the central part of islands of somewhat variable size embedded in an AlTi matrix. We shall assume the presence of a strip of $Al_{11}Ti_7$-like structure along the periphery of such islands. This model is suggested by the high-resolution images, which, moreover, indicate that this band is about one $Al_{11}Ti_7$ unit cell wide.

Along a cross section following a [100] direction one thus encounters one row of structural elements of $Al_{11}Ti_7$ at both ends and in between a variable number of structural elements of Al_5Ti_3. We shall consider islands with sizes such that $q=3$, 4, 5, 7; furthermore, p is assumed to be 4, *i.e.* we assume that there are two periods of $\frac{3}{2}a_0$ along the periphery of the island. The incommensurability then becomes a

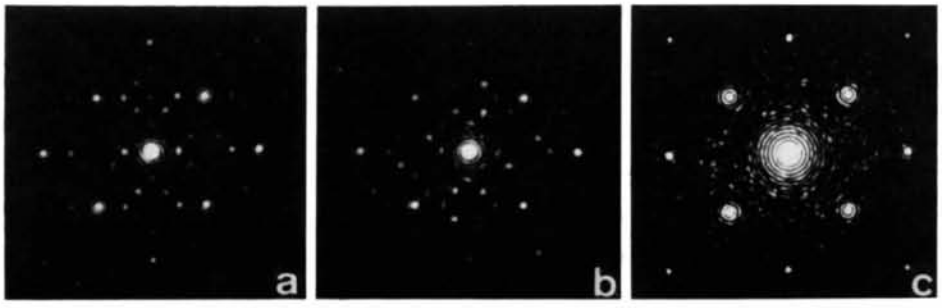

Fig. 7. Selected-area optical diffraction pattern from different areas of the high-resolution image of Fig. 6. (*a*) Core of the island; a commensurate diffraction pattern is obtained. (*b*) Boundary region of an island; incommensurate diffraction pattern. (*c*) The matrix shows the AlTi diffraction pattern only.

simple function of the island size $(q/2)$

$$\delta = [1/2(q+3)](1/a_0).$$

For an infinite island size $\delta = 0$, the smaller the islands, the large the incommensurability (Fig. 9). Intuitively this can be understood by noting that since the thickness of the peripheral layer is assumed to be constant the effect of the core structure increases with its size. The effect of the different spacing in the periphery is more important in small islands than in larger ones.

Measurements on Fig. 3(b) and (c) yield δ values of the order of $(1/30)(1/a_0)$. With the assumption that $p = 4$ this yields core sizes of the order of 7×7 $(2a_0)$ which is in agreement with the actually observed size of approximately 9 nm.

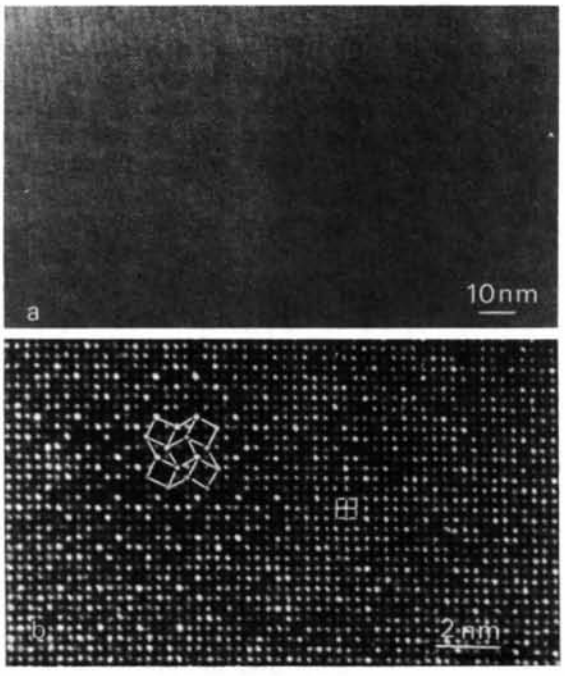

Fig. 8. High-resolution image obtained from a sample producing a different pattern such as Fig. 3(c) (200 kV). (a) Low-magnification image; note that the islands are smaller than in Fig. 6. (b) High-magnification, high-resolution image. The configuration of bright dots consisting of squares and lozenges corresponds to the configuration of Al atoms in the mixed layer of Al_5Ti_3. The squares correspond to the configuration of Al in the AlTi matrix. An example of the lozenge configuration occurring in the hypothetical $Al_{11}Ti_7$ is also indicated.

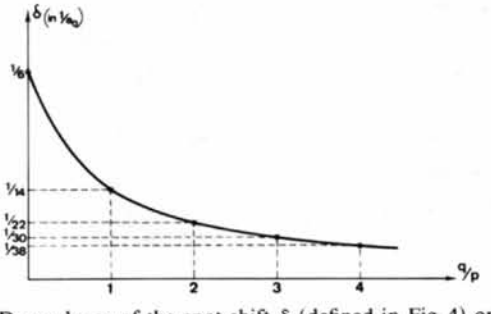

Fig. 9. Dependence of the spot shift δ (defined in Fig. 4) on the island size, *i.e.* the parameter q/p.

7. Structure models and their simulation

In order to simulate the observed electron diffraction patterns as faithfully as possible we constructed optical masks by means of dot patterns representing the Al atoms in the mixed layers of the Al_5Ti_3 structure, as present in the core of the island.

Different sizes were given to this core, containing from three to seven rows of squares of Al atoms along mutually perpendicular directions. This core was surrounded by a structure consisting of rows of squares and lozenges, such as those occurring in the $Al_{11}Ti_7$ structure.

The two structures can be joined along cube planes without violating this building principle; a model for this contact region is represented in Fig. 10. In this region the sequence of {100} Al planes is perturbed. The Al occupancy is indicated schematically by the bars of different thickness. The rows which do not contain Al are spaced $2a_0$ in the core and $\frac{3}{2}a_0$ along the periphery. The model of Fig. 11 was constructed according to this principle. Photographically demagnified images of such dot patterns (omitting the lines of Fig. 11) were used as optical gratings. With an

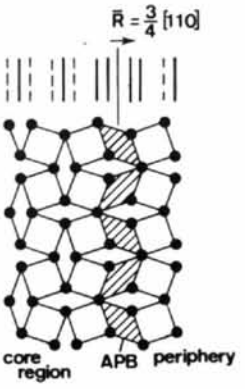

Fig. 10. Model for the transition between the structure in the core of the islands and that in the periphery; only Al positions are shown.

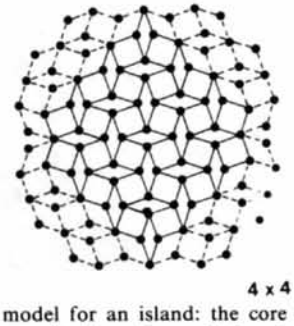

Fig. 11. Typical model for an island: the core has 4×4 Al_5Ti_3 structural elements; its shape is rounded; only Al positions are shown.

argon-ion laser providing the light source optical diffraction patterns were obtained, which are represented in Fig. 12.

The patterns exhibit different degrees of incommensurability depending on the core size.

The largest island (7×7) produces the patterns of Fig. 12 (c) and (d); the latter is practically indistinguishable from that of Al_5Ti_3. The image of Fig. 12(c) is somewhat complicated by the fact that it also exhibits diffraction effects due to the square shape of the Al_5Ti_3 core of the island. On the other hand, the smallest (3×3) island produces the diffraction pattern of Fig. 12(a) for which the δ value is in fair agreement with the formula for an island of the size (see § 6).

Furthermore, when comparing the electron diffraction patterns with the optical ones, one has to be aware of the fact that the former is produced by several islands, whereas the latter originates from a single island as noted above.

We have also constructed a model for a rounded island containing 4×4 rows of squares (Fig. 11). In doing so the above-mentioned artifacts are avoided as can be judged from the optical diffraction pattern in Fig. 12(b).

The non-stoichiometric alloys with a composition in the vicinity of Al_5Ti_3 have a particular texture. The tetragonal two-dimensional long-period superstructure of this alloy, as determined by Miida *et al.* (1982), occurs in the core of small well separated islands ($\sim\leq$20 nm). The matrix surrounding these islands appears to have the $L1_0$ structure of AlTi in specimens exhibiting incommensurate diffraction patterns. The transition region in a band along the periphery of the islands contains a different structure with an intermediate composition in which the interplanar spacing is different from that in the core. It is the presence of this region which causes the incommensurability in the electron diffraction patterns; the incommensurability is related to the chemical composition because of the dependence of the latter on the ratio of the number of 'normal' interplanar spacings to the number of 'deviating' interplanar spacings, which is itself related to the island size.

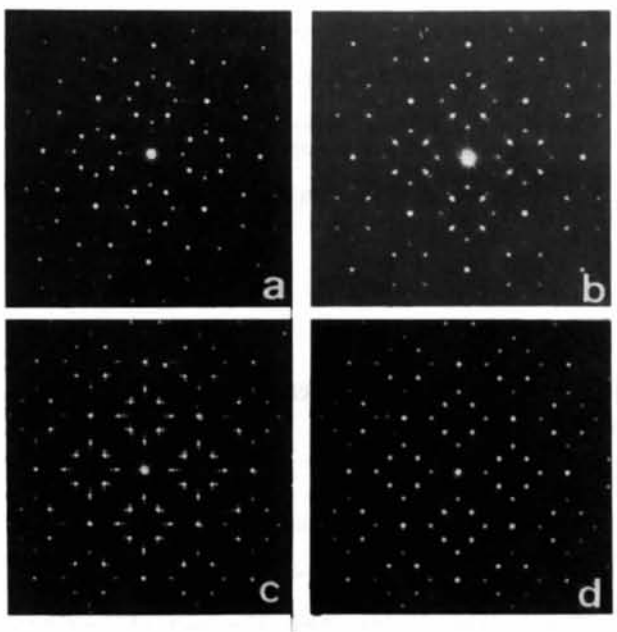

Fig. 12. Optical diffraction patterns obtained from different models: (a) from a 3×3 square island (large δ); (b) from a 4×4 rounded island shown in Fig. 11 (intermediate δ); (c) from a 7×7 square island; the fine structure of the spots is due to the square shape of the island; the δ value is small; (d) from the core of a 7×7 island; the pattern is commensurate.

8. Discussion

The observations presented here strongly suggest that the alloy Al–37 at.% Ti has a heterogeneous structure consisting of small islands embedded in a matrix of $L1_0$ structure with composition AlTi. The core of the islands consists of the two-dimensional long-period superstructure with ideal composition Al_5Ti_3 first reported by Miida *et al.* (1982). A band along the periphery of the islands contains a somewhat different structure, which also exhibits a different period along two, mutually perpendicular, directions. The incommensurability in the diffraction patterns results from the fact that spot positions are determined by the 'average' spacing. A similar incommensurability was found in γ-brass, such as the precipitates observed in the (Cu–Al) alloy; in this case also the incommensurability was attributed to the change in spacing resulting from the presence of non-conservative, non-periodic antiphase boundaries, causing locally a different periodicity (Lovey, Van Tendeloo, Van Landuyt, Chandrasekaran & Amelinckx, 1984).

In fact, the peripheral structure in our model, as represented separately in Fig. 10, can also be considered as being generated from the Al_5Ti_3 structure by introducing a non-conservative antiphase boundary along a cube plane and with a displacement vector $\mathbf{R}=\frac{3}{4}[110]$.

According to this description the islands are surrounded by a peripheral non conservative antiphase boundary, which is not necessarily confined to a single cube plane. In each segment the displacement vector is such as to be perpendicular to the closest cube direction.

The presence of the antiphase boundary introduces different spacings (Fig. 10).

The model presented here explains why the 'incommensurability' is a function of composition.

The observed difference in relative intensity of the 400 reflections in the two isostructural materials Al_5Ti_3 and Ga_5Ti_3 is due to the fact that in Al_5Ti_3 the matrix has the $L1_0$ structure which contributes strongly to this reflection. The alloy Ga_5Ti_3, on the other hand, is homogeneous and a true equilibrium

phase; the entire specimen lights up when making a dark-field image in a superstructure spot. As a result the 400 spot (*i.e.* the $110_{f.c.c.}$ spot) is not reinforced by diffraction from a matrix, as opposed to what is almost inevitably the case in Al_5Ti_3.

The model also explains, of course, why dark-field images in the diffraction contrast mode, made in incommensurate reflections, reveal the islands as bright patches.

The size of these islands is to a large extent independent of the annealing temperature but decreases with increasing deviations from the stoichiometric composition.

A similar phenomenon was observed by some of the present authors (Den Broeder *et al.*, 1981) in Cr-Al alloys at compositions between 26 and 33 at.% Al. Here a phase called *X* with composition close to Cr_5Al_3 was observed which, in spite of very long annealing times, remained in an embryonic size range of 3-5 nm; the influence of composition on island size was less pronounced here.

The model also explains why even in nominally stoichiometric Al_5Ti_3 some $TiAl_2$ precipitates are still found. The stoichiometric compound only exists in small islands, the rest of the specimen contains Al_2Ti and TiAl; the first one contains an excess of Al whereas the second contains an excess of Ti.

When irradiating a sample containing Al_5Ti_3 islands as well as Al_2Ti precipitates in a matrix of AlTi it is found that Al_5Ti_3 is preferentially disordered. The superstructure reflections due to Al_5Ti_3 disappear rapidly whereas the diffraction spots due to the Al_2Ti and AlTi remain (Fig. 3*d*). These observations suggest that Al_5Ti_3 is a less stable structure than Al_2Ti and AlTi.

9. Conclusions

In the present paper we have tried to explain the incommensurability in the electron diffraction patterns by assuming a core region with structure *A* surrounded by a thin boundary region having a structure *B*. If this boundary area becomes very narrow (in terms of the unit cell which is here $1{\cdot}1 \times 1{\cdot}1$ nm) it is difficult to define the structure *B* and it becomes equally justified to describe the island as consisting completely of structure *A* but containing a single antiphase boundary close to the border. The schematic representation of Fig. 10 can be readily interpreted in this way. The diffraction effects associated with a single APB in a small crystal as well as those associated with a set of small islands all containing APB's of the same type have been extensively analyzed in a recent paper by Van Dyck *et al.* (1984).

In the particular model considered here the approach used in the present paper and that used by Van Dyck *et al.* (1984) lead to consistent results.

Part of the experimental work was carried out at the National Center for Electron Microscopy at LBL Berkeley. We would like to thank Prof. G. Thomas, R. Gronsky and K. Westmacott for the use of their facilities.

References

DEN BROEDER, F. J. A., VAN TENDELOO, G., AMELINCKX, S., HORNSTRA, J., DE RIDDER, R., VAN LANDUYT, J. & VAN DAAL, H. J. (1981). *Phys. Status Solidi A*, **67**, 233-248.

FUJIWARA, K. (1957). *J. Phys. Soc. Jpn*, **12**, 7-13.

LOISEAU, A. & LASALMONIE, A. (1983). *Acta Cryst* B**39**, 580-587.

LOVEY, F. C., VAN TENDELOO, G., VAN LANDUYT, J., CHANDRASEKARAN, M. & AMELINCKX, S. (1984). *Acta Metall.* **32**, 879-886.

MIIDA, R., HASHIMOTO, S. & WATANABE, D. (1982). *Jpn. J. Appl. Phys.* **21**, L59-L61.

VAN DYCK, D. (1980). *J. Microsc.* **119**, 141-152.

VAN DYCK, D., VAN TENDELOO, G. & AMELINCKX, S. (1984). *Ultramicroscopy*, **15**, 357-370.

VAN TENDELOO, G. & AMELINCKX, S. (1978). *Phys. Status Solidi A*, **47**, 555-564.

Acta Cryst. (1985). B**41**, 418-425

The Solution of Unknown Crystal Structures from X-ray Powder Diffraction Data. Technique and an Example, $ZrNaH(PO_4)_2$

BY PHIL RUDOLF AND ABRAHAM CLEARFIELD*

Chemistry Department, Texas A&M University, College Station, Texas 77843, *USA*

(*Received* 27 *August* 1984; *accepted* 11 *February* 1985)

Abstract

An integrated system whereby the structure of an unknown polycrystalline compound can be solved from X-ray powder data, collected on a powder diffractometer, is described. The method developed falls into three main sections: accurate data collection and analysis of the pattern to give unit-cell parameters and space group; structure analysis, *via* Patterson/direct methods and Fourier/difference Fourier techniques using integrated intensities of unam-

* To whom correspondence should be addressed.

0108-7681/85/060418-08$01.50